An ortholog of the Vasa intronic gene is required for small RNA-mediated translation repression in *Chlamydomonas reinhardtii*

Xinrong Ma[a,b,1,2], Fadia Ibrahim[a,b,1,3], Eun-Jeong Kim[a,b,4], Scott Shaver[a,b], James Becker[a,b], Fareha Razvi[a,b], Ronald L. Cerny[c], and Heriberto Cerutti[a,b,5]

[a]School of Biological Sciences, University of Nebraska–Lincoln, Lincoln, NE 68588; [b]Center for Plant Science Innovation, University of Nebraska–Lincoln, Lincoln, NE 68588; and [c]Department of Chemistry, University of Nebraska–Lincoln, Lincoln, NE 68588

Edited by Xuemei Chen, University of California, Riverside, CA, and approved December 2, 2019 (received for review May 14, 2019)

Small RNAs (sRNAs) associate with Argonaute (AGO) proteins in effector complexes, termed RNA-induced silencing complexes (RISCs), which regulate complementary transcripts by translation inhibition and/or RNA degradation. In the unicellular alga *Chlamydomonas*, several metazoans, and land plants, emerging evidence indicates that polyribosome-associated transcripts can be translationally repressed by RISCs without substantial messenger RNA (mRNA) destabilization. However, the mechanism of translation inhibition in a polyribosomal context is not understood. Here we show that *Chlamydomonas* VIG1, an ortholog of the *Drosophila melanogaster* Vasa intronic gene (VIG), is required for this process. VIG1 localizes predominantly in the cytosol and comigrates with monoribosomes and polyribosomes by sucrose density gradient sedimentation. A *VIG1*-deleted mutant shows hypersensitivity to the translation elongation inhibitor cycloheximide, suggesting that VIG1 may have a nonessential role in ribosome function/structure. Additionally, FLAG-tagged VIG1 copurifies with AGO3 and Dicer-like 3 (DCL3), consistent with it also being a component of the RISC. Indeed, VIG1 is necessary for the repression of sRNA-targeted transcripts at the translational level but is dispensable for cleavage-mediated RNA interference and for the association of the AGO3 effector with polyribosomes or target transcripts. Our results suggest that VIG1 is an ancillary ribosomal component and plays a role in sRNA-mediated translation repression of polyribosomal transcripts.

microRNA | RNA interference | SERBP1 | RNA silencing | VIG1

Several classes of small RNAs (sRNAs) have been recognized in diverse eukaryotes and play essential roles in a broad array of biological processes (1–5). MicroRNAs (miRNAs) are generally processed, by RNase III enzymes such as Dicer, from imperfectly paired stem-loop regions of single-stranded endogenous RNAs, whereas small interfering RNAs (siRNAs) are produced from long, near-perfectly complementary double-stranded RNAs (dsRNAs) of various origins (1–5). These sRNAs are incorporated into effector complexes, known as (micro)RNA-induced silencing complexes ([mi]RISCs), which contain Argonaute (AGO) proteins as core components (1–5). AGOs bind sRNAs and use them as guides to identify complementary sequences in nucleic acids targeted for silencing. Highly complementary sRNA–mRNA hybrids often trigger AGO-mediated endonucleolytic cleavage of transcripts, the best-characterized mechanism of posttranscriptional gene silencing mediated by siRNAs and, in land plants, by many miRNAs (1, 2, 4). Conversely, imperfect sRNA–mRNA hybrids, with central bulges or mismatches, frequently lead to translation inhibition and/or exonucleolytic (AGO "slicer"-independent) transcript decay (1, 3–5). However, recent evidence indicates that sRNAs perfectly complementary to a target mRNA can also cause translation repression (2, 4, 6). This outcome may result from the association of sRNAs with AGOs that lack endonucleolytic activity or from modulation of the AGO endonucleolytic activity by posttranslational modifications and/or by interaction with ancillary factors in an (mi)RISC (3, 4, 6).

Substantial progress has been made in our understanding of the mechanisms of miRNA-mediated posttranscriptional gene silencing. In metazoans, AGO-miRNA binding to the 3′ untranslated region (UTR) of a target transcript recruits a glycine-tryptophan repeat-containing protein (GW182 or TNRC6). GW-repeat proteins interact with the cytoplasmic poly(A)-binding protein, associated with the mRNA poly(A) tail, and with the CCR4–NOT and PAN2–PAN3 deadenylase complexes (1, 3–5). CCR4–NOT, in turn, recruits the RNA helicase DDX6, which is thought to play an important role in translation repression (1, 3–5). The coordinated action of these proteins results in inhibition of cap-dependent translation, at an initiation step, and transcript deadenylation, eventually causing mRNA degradation through decapping and 5′-to-3′ exonucleolytic decay (1, 3–5). Genome-wide proteomic and transcriptomic analyses, after the removal or the ectopic expression

Significance

Small RNAs (sRNAs) are a class of noncoding RNAs that regulate complementary mRNAs, by triggering translation repression and/or transcript decay, and influence multiple biological processes. In animals, land plants, and some protists like the alga *Chlamydomonas*, sRNAs can repress translation of polyribosome-associated mRNAs, without or with only minimal transcript destabilization. However, the precise silencing mechanism is poorly understood. We found that *Chlamydomonas* VIG1, a homolog of the *Drosophila melanogaster* Vasa intronic gene and a member of a widely conserved protein family in eukaryotes, is involved in this process. VIG1 appears to be an ancillary ribosomal constituent. Additionally, VIG1 copurifies with core components of sRNA effector complexes and plays a key role in the sRNA-mediated translation repression of polyribosomal transcripts.

Author contributions: X.M., F.I., and H.C. designed research; X.M., F.I., E.-J.K., S.S., J.B., and F.R. performed research; R.L.C. contributed new reagents/analytic tools; X.M., F.I., E.-J.K., S.S., R.L.C., and H.C. analyzed data; and H.C. wrote the paper.

The authors declare no competing interest.

This article is a PNAS Direct Submission.

[1]X.M. and F.I. contributed equally to this work.

[2]Present address: State Key Laboratory of Food Nutrition and Safety, Tianjin University of Science & Technology, 300457 Tianjin, People's Republic of China.

[3]Present address: Department of Pathology and Laboratory Medicine, Division of Neuropathology, Perelman School of Medicine, University of Pennsylvania, Philadelphia, PA 19104.

[4]Present address: Department of Life Science, Chung-Ang University, 06974 Seoul, Korea.

[5]To whom correspondence may be addressed. Email: hcerutti1@unl.edu.

This article contains supporting information online at https://www.pnas.org/lookup/suppl/doi:10.1073/pnas.1908356117/-/DCSupplemental.

First published December 23, 2019.

of miRNAs, suggest that this slicer-independent degradation of target transcripts may account for most of the miRNA-mediated stable repression in many postembryonic cells (1, 4, 5).

In contrast, in embryonic stem cells and during early embryogenesis of metazoans, miRISC binding to target messenger RNAs (mRNAs) mainly causes translation inhibition, with little effect on transcript stability (1, 7, 8). Similar observations have been reported in neurons, where reversible miRISC-mediated silencing regulates synaptic plasticity (9). Intriguingly, GW-repeat proteins are absent from the miRISC in the *Caenorhabditis elegans* germline (7) and from the polyribosome-associated miRISC that strongly inhibits translation upon serum starvation in *Drosophila melanogaster* S2 cells (10). Moreover, in somatic mammalian cell lines, certain miRNAs binding to the protein-coding sequence (CDS) of transcripts repress translation, through a GW182/TNRC6-independent mechanism, without triggering mRNA destabilization (11). Thus, in metazoans, miRNAs appear to regulate target transcripts via several mechanisms that can be modulated by cellular context, miRISC composition, and subcellular localization, as well as target mRNA-specific effects (4, 12, 13).

In land plants, even the slicer mode of miRNA action appears to target (many) translating mRNAs. By isolating poly(A) RNAs having a 5′ monophosphate (as a result of RNA cleavage/degradation) and identifying the nucleotide positions of the 5′ ends, a 3-nt periodicity in the RNA degradation products within the CDS was observed for a number of miRNA targets, suggesting that 5′-to-3′ degradation accompanies the codon-by-codon translocation of elongating ribosomes (2, 14). This is consistent with findings that AGO1 and miRNAs associate with polyribosomes in *Arabidopsis thaliana* (2, 4). In this species, several miRNAs with a high degree of sequence complementarity to target transcripts can trigger both mRNA cleavage and translation repression (2, 4, 15). Plants and green algae lack orthologs of the metazoan GW182/TNRC6 proteins and, in *A. thaliana*, the known factors required for miRNA-mediated translation inhibition include the microtubule-severing enzyme KATANIN1, decapping enhancer VARICOSE, GW-containing protein SUO, endoplasmic reticulum (ER) membrane protein ALTERED MERISTEM PROGRAM1, and dsRNA-binding protein DRB2 (2, 4, 15, 16). Subcellular localization and fractionation studies indicated that miRNA-mediated translation repression mainly occurs on membrane-bound polyribosomes, likely associated with the ER (2, 4, 15). Studies with lysates from tobacco BY-2 cells suggested that the plant (mi)RISC, bound to the 5′ UTR or the CDS of a transcript, can sterically block the recruitment or the movement of ribosomes (17). However, a preferential accumulation of ribosome footprints was not observed in the region upstream of CDS miRNA target sites in *A. thaliana* Ribo-seq (sequencing) or RNA degradome data (14, 18).

Translation inhibition mediated by sRNAs also occurs in *C. reinhardtii* (6, 19, 20) and the translationally repressed transcripts remain associated with polyribosomes (6). Global ribosome profiling in parallel with RNA-seq and quantitative proteomics on a Dicer mutant and its Dicer-complemented strain revealed that *Chlamydomonas* miRNAs regulate endogenous targets mainly by pairing to the CDS of transcripts, leading to RNA degradation and/or translation repression (20). However, ribosome footprints were not piled up upstream of the miRNA-binding sites (20). Thus, sRNA-mediated translation repression of polyribosome-associated transcripts is a widespread phenomenon in eukaryotes but the actual molecular mechanism(s) remains largely uncharacterized. Here, we show that a *Chlamydomonas* ortholog of the *D. melanogaster* Vasa intronic gene (VIG) and mammalian SERPINE1 mRNA-binding protein 1 (SERBP1) is required for translation repression mediated by siRNAs/miRNAs. *Chlamydomonas* VIG1 is a component of the (mi)RISC, associates with translating ribosomes in an mRNA-independent manner, and may possibly modulate multiple steps of protein synthesis.

Results

VIG1 Is Required for Translation Repression Mediated by siRNAs/miRNAs. In *C. reinhardtii*, the tryptophan synthase β-subunit (TSβ; encoded by the *MAA7* gene) is required to convert the indole analog 5-fluoroindole (5-FI) into the toxic tryptophan analog 5-fluorotryptophan. Suppression of *MAA7* by RNA interference (RNAi), triggered by dsRNAs produced from inverted-repeat (IR) transgenes, results in strains resistant to 5-FI (6, 21). In

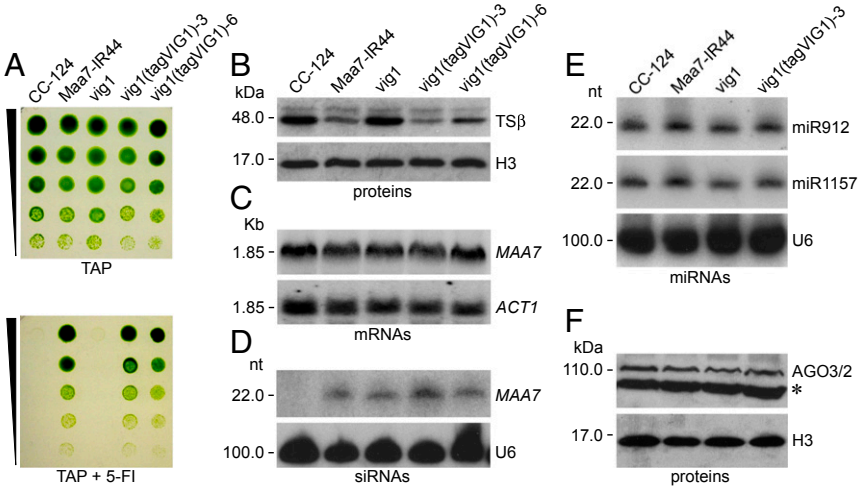

Fig. 1. *Chlamydomonas* VIG1 is required for the siRNA-mediated translation repression of the *MAA7* transcript. (*A*) Growth and survival of the indicated strains on TAP medium with or without 7 μM 5-fluoroindole. CC-124, wild-type strain; Maa7-IR44, CC-124 transformed with an IR transgene designed to induce RNAi of *MAA7*; vig1, *VIG1* deletion mutant; vig1(tagVIG1)-3 and -6, transgenic strains of vig1 transformed with FLAG-CBP-VIG1 under the control of the *PsaD* promoter. (*B*) Immunoblot analysis of tryptophan synthase β-subunit levels. Immunodetection of histone H3 was used as a control for equivalent loading of the lanes. (*C*) Northern blot analysis of *MAA7* transcript levels. The same filter was reprobed with the coding sequence of *ACT1* (encoding actin) as a control for similar loading of the lanes. (*D*) Northern blot analysis of *MAA7* siRNAs in the indicated strains. The same filter was reprobed with the U6 small nuclear RNA sequence to assess the amount of sample loaded per lane. (*E*) Northern blot analyses of sRNAs isolated from the indicated strains and detected with probes specific for *Chlamydomonas* miRNAs. (*F*) Immunoblot analysis of AGO3/2 proteins in the indicated strains. The asterisk indicates a nonspecific cross-reacting antigen.

several transgenic strains, like Maa7-IR44, *MAA7* is silenced by siRNA-mediated translation repression of polyribosome-associated transcripts, without mRNA destabilization (6). In order to gain some insights into this process, we generated a library of RNAi-defective insertional mutants in the Maa7-IR44 background. One such mutant, designated *vig1*, contained a deletion of the *Cre09.g393358* (*VIG1*) gene, encoding the only *Chlamydomonas* member of a conserved eukaryotic protein family that includes VIG and SERBP1 (*SI Appendix*, Figs. S1*A* and S2). The entire *VIG1* gene is deleted in *Chlamydomonas vig1* (*SI Appendix*, Fig. S3*A*) and no *VIG1* transcript is detected, by Northern blotting, in the mutant background (*SI Appendix*, Fig. S3*B*).

The *vig1* mutant showed sensitivity to 5-FI, indicating a defect in the RNAi-mediated suppression of *MAA7* (Fig. 1*A*). Moreover, it contained TSβ-protein amounts quite similar to those in the wild-type CC-124 strain (Fig. 1*B*), without appreciable changes in the *MAA7* transcript abundance (Fig. 1*C*). *MAA7* siRNA levels were slightly reduced in the mutant background (Fig. 1*D*), as were the amounts of a few miRNAs (Fig. 1*E*) and of AGO3/2 (Fig. 1*F*), the main core components of the (mi)RISC in *Chlamydomonas* (19). However, the barely noticeable reduction in components of the RNAi machinery seemed insufficient to explain the defect in siRNA-mediated translation repression of *MAA7*. Transformation of the *vig1* mutant with a transgene stably expressing FLAG-CBP–tagged VIG1 (*Materials and Methods*) reverted all described phenotypes (Fig. 1).

We also examined how the deletion of *VIG1* affected the expression of *Chlamydomonas* genes regulated by endogenous miRNAs/siRNAs. We already demonstrated that *Cre16.g683650* (encoding a predicted protein kinase) is translationally repressed by the miR_C sRNA (22). The miR_C binding site in the *Cre16.g683650* mRNA overlaps the stop codon and contains a mismatch with

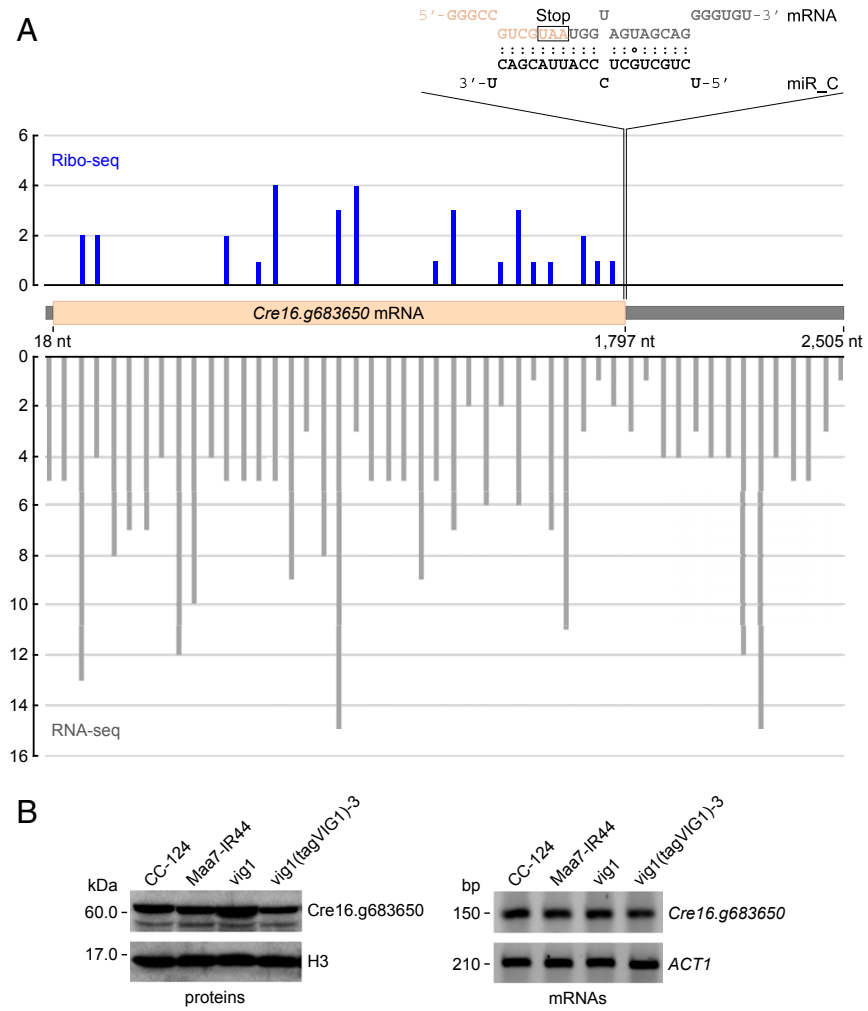

Fig. 2. *Chlamydomonas vig1* mutant is defective in the translation repression, by an endogenous miRNA, of *Cre16.g683650* (encoding a predicted protein kinase of unknown function). (*A*) Ribosome profiling of the *Cre16.g683650* transcript. The diagram (*Top*) depicts the hybridization of miR_C to its recognition site, overlapping the stop codon, in the *Cre16.g683650* mRNA. The mismatch to nucleotide 10 of the miRNA would prevent AGO-mediated cleavage of the target transcript. Histograms of the 5′-end positions of ribosome-protected fragments (Ribo-seq; blue) or of normalized total RNA reads (RNA-seq; gray) are shown along the length of the mRNA schematic (CDS is indicated by the orange box). Ribosome-protected fragments were predominantly 27 (or 28) nt in length and their 5′ ends mapped to the second (or first) nucleotide position of codons, consistent with previous genome-wide Ribo-seq analyses in *Chlamydomonas* (56). The distribution on the transcript of RNA-seq reads serves as a control for a possible technical bias in the detection of certain mRNA sequences. The *y* axes of the histogram graphs indicate read frequency. (*B*) Immunoblot and semiquantitative RT-PCR analyses of *Cre16.g683650* protein and transcript levels in the indicated strains. Immunodetection of histone H3 was used as a control for equivalent loading of proteins in the lanes. Amplification of *ACT1* (encoding actin) transcripts is shown as an RT-PCR input control. CC-124, wild-type strain; Maa7-IR44, CC-124 transformed with an IR transgene designed to induce RNAi of *MAA7*; vig1, *VIG1* deletion mutant; vig1(tagVIG1)-3, transgenic strain of vig1 transformed with FLAG-CBP-VIG1 under the control of the *PsaD* promoter.

nucleotide 10 of the sRNA, which would hinder AGO-mediated cleavage (Fig. 2*A*). As with *MAA7*, *Cre16.g683650* was translationally derepressed in the *vig1* mutant without any obvious alteration in its transcript level (Fig. 2*B*). In contrast, the regulation of 2 mRNAs, corresponding to *Cre17.g697550* and *Cre12.g552950*, targeted for cleavage by *Chlamydomonas* miRNAs and/or endogenous siRNAs (22, 23) was not defective in the mutant background. Their transcript abundance did not change in *vig1* relative to the wild-type or the complemented strains (*SI Appendix*, Fig. S4*A*). In addition, the steady-state levels of several miRNAs, including miR_C, and of the transcripts for the 3 AGOs encoded in the *Chlamydomonas* genome were not substantially altered in the *vig1* mutant (*SI Appendix*, Fig. S4 *B* and *C*).

These results, taken together, suggest that *Chlamydomonas* VIG1 is required for sRNA-mediated translation repression but seems entirely dispensable for sRNA-mediated target RNA cleavage/degradation. We have previously reported that sRNA-repressed transcripts were found associated with polyribosomes by sucrose density gradient centrifugation (6). Although ribosome-profiling data on individual transcripts tend to be noisy without very deep coverage, we nevertheless also examined, by Ribo-seq, the association with ribosomes of the miR_C translationally repressed *Cre16.g683650* transcript. Ribosome-protected mRNA fragments (RPFs) of typical length distribution and with the 3-nt periodicity indicative of translationally active ribosomes were clearly detected (Fig. 2*A*). Moreover, the RPFs were fairly uniformly spread along the CDS, without any obvious ribosome stalling upstream of the miR_C binding site (Fig. 2*A*).

VIG1 Copurifies with (mi)RISC Core Components. VIG/SERBP1 has been previously identified as a component of the (mi)RISC in *D. melanogaster*, *C. elegans*, and human cells (24, 25). However, its role has remained somewhat enigmatic since its down-regulation caused a slight (cleavage-mediated) RNAi defect in *D. melanogaster* and no obvious RNAi deficiency in *C. elegans* (24). To explore whether *Chlamydomonas* VIG1 might be an (mi)RISC component, we affinity purified FLAG-CBP–tagged VIG1 from RNase A-treated cell lysates of a complemented *vig1* transgenic strain and identified associated proteins by mass spectrometry (Fig. 3*A*). As a negative control, we carried out similar purifications from a transgenic strain expressing a FLAG-CBP–tagged bleomycin resistance protein (Ble) from *Streptoalloteichus hindustanus*. In 3 independent experiments, VIG1 copurified with AGO3 and DCL3 (Fig. 3*A* and *SI Appendix*, Table S1), 2 well-characterized core RNAi components in *Chlamydomonas* (19, 20, 22). In addition, VIG1 associated, in at least 2 experiments, with putative mRNA splicing factors (SART1, squamous cell carcinoma antigen recognized by T cells 1; SRP23, serine arginine rich-like protein 23), several components of the protein translation machinery (eIF3A, eukaryotic translation initiation factor 3 subunit A; eIF3M, eukaryotic translation initiation factor 3 subunit M; eIF4A, eukaryotic translation initiation factor 4 subunit A; eS4 [RPS4], 40S ribosomal protein S4e; eS7 [RPS7], 40S ribosomal protein S7e; eL13 [RPL13], 60S ribosomal protein L13e; uL13 [RPL13A], 60S ribosomal protein L13A), a putative ATP-dependent RNA helicase (HEL61), and protein arginine *N*-methyltransferase 2 (PRMT2) (Fig. 3*A* and *SI Appendix*, Table S1). The associations appear to be specific, since none of these proteins was detected in 3 equivalent purifications with FLAG-CBP-Ble, and RNA-independent, since the cell lysates were treated with RNase A.

The (mi)RISC can catalyze the endonucleolytic cleavage of RNA substrates, as directed by complementarity to its associated siRNAs/miRNAs. Since FLAG-CBP-VIG1 and associated proteins were purified from cells containing *MAA7* siRNAs, which we have previously characterized by sequencing (6, 21), we designed a complementary *MAA7* RNA substrate to test whether the isolated complex showed sequence-specific nuclease activity in vitro. In this assay, expected cleavage products were observed for the full reactions with or without ATP (Fig. 3*B*). However, the endonucleolytic activity was abolished by the addition of EDTA, which chelates the Mg^{2+} cofactors required for AGO slicer activity. As controls, no specific cleavage was observed by incubation of the homologous RNA substrate with FLAG-CBP-Ble or

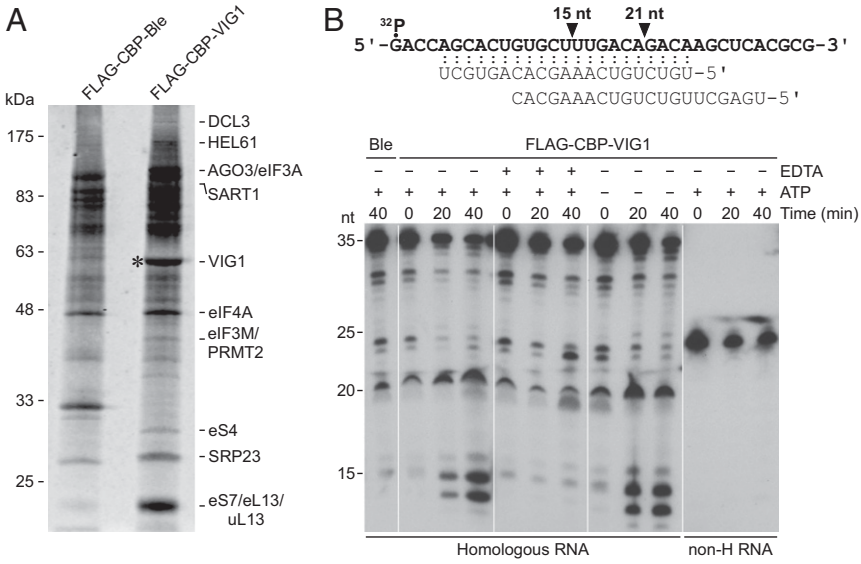

Fig. 3. VIG1 is a bona fide (mi)RISC component. (*A*) FLAG-CBP-VIG1–associated proteins, isolated by affinity purification, were separated by SDS/PAGE and visualized by Sypro Ruby staining. The indicated proteins were identified by mass spectrometry analyses. A mock purification with FLAG-CBP–tagged Ble (conferring resistance to bleomycin) is also shown. The asterisk indicates the FLAG-CBP-VIG1 protein. (*B*) In vitro RISC cleavage assay. The diagram (*Top*) depicts the homologous RNA substrate, hybridizing to 2 fully complementary *MAA7* siRNAs, and the predicted cleavage sites generating ^{32}P-labeled 5′-RNA fragments of the indicated lengths. FLAG-CBP-VIG1 and associated proteins were affinity purified and incubated with the homologous RNA or with a nonhomologous RNA (non-H RNA) under the denoted conditions. Reaction products were separated on a denaturing polyacrylamide/urea gel and analyzed by autoradiography (*Bottom*). The homologous RNA substrate was also incubated with purified FLAG-CBP-Ble as a negative control.

by incubation of a nonhomologous RNA substrate with FLAG-CBP-VIG1 (Fig. 3*B*). Thus, *C. reinhardtii* VIG1 appears to be an (mi)RISC component, part of a complex with AGO3 that is capable of siRNA-directed sequence-specific RNA cleavage. It is possible, but currently untested, that VIG1 may affect to some degree (mi)RISC loading/stability, explaining the very minor reduction in AGO3/2 and certain siRNA/miRNA levels in the *vig1* strain (Fig. 1 *D*–*F*). However, it is unlikely that VIG1 is required for target RNA cleavage since, as already mentioned, its absence in the *vig1* mutant does not result in deficient regulation of endogenous sRNA targets subject to cleavage/degradation (*SI Appendix*, Fig. S4*A*). Interestingly, in its normal cellular context, the RISC represses the *MAA7* transcript at the translational level without mRNA cleavage/degradation (Fig. 1*C*). In contrast, the in vitro purified RISC can cleave an *MAA7* homologous RNA (Fig. 3*B*). We speculate that some associated factor(s) and/or posttranslational modification(s), which might suppress AGO3 endonucleolytic activity in vivo, may have been lost during the purification.

VIG1 Is Mainly Located in the Cytosol and Associates with Bona Fide Translating Ribosomes. VIG1 is predicted to be a structurally disordered protein, with intrinsically disordered regions covering ~83% of the polypeptide length (*SI Appendix*, Fig. S1*B*). Some of these regions consist of arginine/glycine-rich (RG/RGG) repeats (*SI Appendix*, Fig. S1*A*). However, 2 sequence domains are well-conserved in putative VIG1 orthologs from a wide spectrum of eukaryotes: the Stm1_N domain, found in the *Saccharomyces cerevisiae* suppressor of Tom 1 (Stm1) protein (*SI Appendix*, Figs. S1*A* and S5), and the HABP4/SERBP1 (PAI-RBP1) domain, found in the HABP4 family of hyaluronan-binding proteins and in SERBP1 (*SI Appendix*, Figs. S1*A* and S6). Cryo-EM structures of eukaryotic 80S ribosomes revealed that yeast Stm1, *D. melanogaster* VIG2, and mammalian SERBP1 interact directly with inactive ribosomes (26, 27). Stm1 and SERBP1 have been proposed to function as clamping factors that prevent ribosome subunit disassembly and preclude their degradation when translation is massively slowed down under nutrient deprivation/stress conditions (27–30).

To begin assessing the association of *Chlamydomonas* VIG1 with ribosomes, we examined its subcellular localization by immunofluorescence imaging. FLAG-CBP-VIG1 was found to localize mainly in the cytosol, with some preference for perinuclear regions (Fig. 4 and *SI Appendix*, Fig. S7). The parental Maa7-IR44 strain was used as a negative control, to verify the absence of background fluorescence in the Alexa Fluor 488 channel corresponding to FLAG-CBP-VIG1. We also tested conditions that might potentially alter VIG1 localization, by virtue of its association with the (mi)RISC and/or with ribosomes. Heat stress triggers translational arrest and the formation of stress granules, cytoplasmic aggregates of stalled translational preinitiation complexes (which can include 40S ribosomal subunits and translation initiation factors), after polyribosome disassembly (31). In contrast, cycloheximide treatment "freezes" translating ribosomes on transcripts (6, 32). However, the localization of FLAG-CBP-VIG1 did not change appreciably under any of the conditions analyzed (Fig. 4 and *SI Appendix*, Fig. S7).

To examine the possible association of VIG1 with translating ribosomes, we carried out polyribosome profiling by sucrose density gradient sedimentation. A fraction of VIG1 comigrated with monoribosomes and polyribosomes, suggesting that VIG1 does associate with actively translating ribosomes (Fig. 5*A*). Interestingly, a fraction of AGO3/2 also comigrated with polyribosomes (Fig. 5*A*),

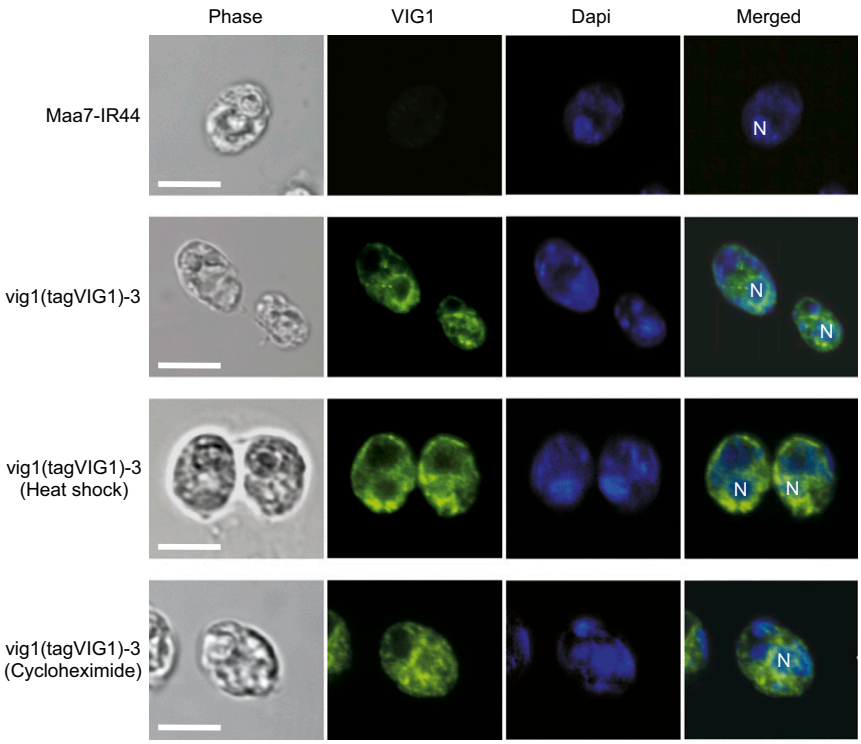

Fig. 4. Immunofluorescence localization of FLAG-CBP–tagged VIG1. Phase-contrast images of the cells, immunolocalization of epitope-tagged VIG1 (detected with an antibody conjugated to Alexa Fluor 488), DAPI staining of nuclear and organellar DNA, and merged images. Representative images are shown, with the location of the nucleus indicated by "N." Cells were grown to middle logarithmic phase in TAP medium, collected by centrifugation, and then processed for immunofluorescence microscopy. Aliquots of cells were also exposed to 42 °C for 45 min (heat shock) or incubated in the presence of 50 μg/mL cycloheximide for 2 h prior to preparation for immunofluorescence microscopy. vig1(tagVIG1)-3, *VIG1* deletion mutant expressing a transgene of FLAG-CBP-VIG1 under the control of the *PsaD* promoter. Maa7-IR44, parental strain. (Scale bars, 5 μm.)

supporting a connection of the (mi)RISC with translating ribosomes and consistent with the previously reported association of sRNAs with polyribosomes (6). To determine further whether the fast-sedimenting VIG1 and AGO3/2 were indeed associated with polyribosomes, we treated lysates with EDTA, known to chelate Mg^{2+} and dissociate translating cytosolic ribosomes into their 40S and 60S subunits (6). This caused, as expected, redistribution of all tested proteins to the subpolyribosomal region of the gradient (*SI Appendix*, Fig. S8*A*). Thus, VIG1 localizes predominantly in the cytosol of *C. reinhardtii* and associates with monoribosomes and polyribosomes.

VIG1 Appears to Be an Auxiliary Protein of Translating Ribosomes but Is Not Required for AGO3 Interaction with Polyribosomes or Target Transcripts. In wild-type *C. reinhardtii*, VIG1 is an abundant protein, similar in relative levels to ribosomal proteins and at least 15 times more abundant than AGO3 (*SI Appendix*, Fig. S9*A*). This implies that the majority of cellular VIG1 is unlikely to be part of the (mi)RISC. The affinity-purification experiments indicated that VIG1 interacts (directly or indirectly but in an RNA-independent manner) with several translation initiation factors and ribosomal proteins (Fig. 3*A*). Additionally, the *vig1* mutant is hypersensitive to exposure to cycloheximide, which inhibits translation elongation (6), but shows lower sensitivity to exposure to hygromycin B or rapamycin (*SI Appendix*, Fig. S9*B*). Hygromycin B seems to affect decoding fidelity as well as translocation of mRNA and tRNAs on the ribosome (6), whereas rapamycin is an inhibitor of the mTOR (mechanistic target of rapamycin) kinase. Together with the described VIG1 comigration with mono/polyribosomes on sucrose density gradients (Fig. 5*A*), these observations suggested that this protein may have an ancillary role(s) in ribosome function/structure (besides being a putative

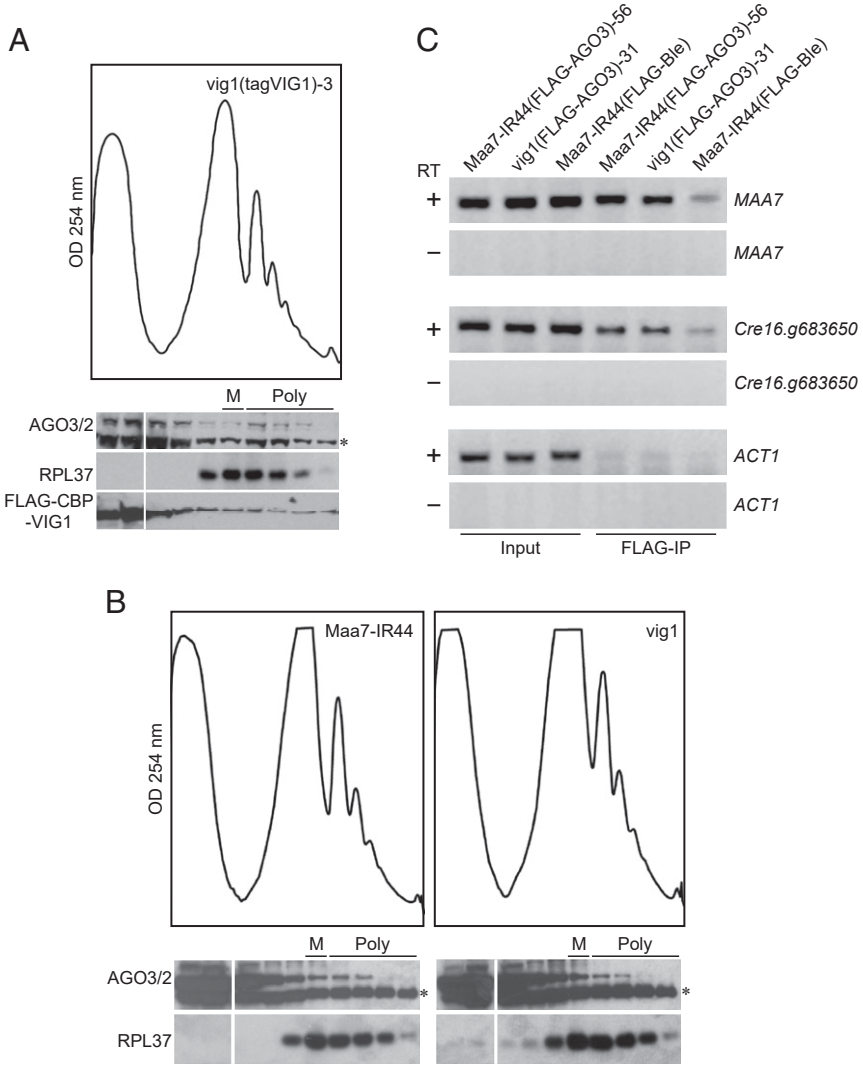

Fig. 5. VIG1 is not required for AGO3 association with polyribosomes or target transcripts. (*A*) Polyribosome profile of a vig1(tagVIG1)-3 lysate treated with 150 μg/mL cycloheximide and fractionated by sucrose density gradient centrifugation (*Top*). The distribution of the AGO3/2, RPL37, and FLAG-CBP-VIG1 proteins in the gradient fractions was examined by immunoblotting (*Bottom*). The location of monoribosomes (M) and polyribosomes (Poly) in the profile is shown above the blots. The asterisk indicates a nonspecific cross-reacting antigen. (*B*) Polyribosome profiles of the Maa7-IR44 and vig1 strains and immunological detection of AGO3/2 and RPL37 distribution in the gradient fractions. (*C*) RNA-binding protein immunoprecipitation and subsequent RT-PCR detection of AGO3-associated transcripts. RIP with anti–FLAG-M2 agarose beads (FLAG-IP) was performed from lysates of the indicated strains. Input RNA corresponded to 5% of the total purified amount. *ACT1* was examined as a control transcript, not targeted by an sRNA-mediated mechanism. Maa7-IR44(FLAG-AGO3)-56, transgenic strain of Maa7-IR44 transformed with FLAG-tagged AGO3; vig1(FLAG-AGO3)-31, transgenic strain of vig1 transformed with FLAG-tagged AGO3; Maa7-IR44(FLAG-Ble), transgenic strain of Maa7-IR44 transformed with FLAG-tagged Ble.

[mi]RISC component). A nonessential role of VIG1 in ribosome function is supported by the fact that overall protein abundance did not change appreciably in the *vig1* mutant relative to the wild-type or the complemented strains (*SI Appendix*, Fig. S10). Moreover, under standard laboratory conditions in TAP (Tris-acetate-phosphate) medium, lack of VIG1 does not appear to affect cell growth (Fig. 1*A* and *SI Appendix*, Fig. S9*B*), suggesting that VIG1 may only play a minor role (if any) in general protein synthesis.

To examine in more detail the function of VIG1 in sRNA-mediated translation inhibition, we tested whether it was required for association of AGO3/2 with polyribosomes or with translationally repressed target RNAs. However, the distribution of AGO3/2 by sucrose gradient sedimentation was very similar in both *vig1* and its parental strain (Fig. 5*B*), suggesting that AGO3/2 interaction with polyribosomes is VIG1-independent. Our anti-AGO3/2 antibody was raised against an AGO3 peptide (21) but, in immunoblots, it also recognizes the much less abundant AGO2 homolog (19). However, its binding affinity appears to be too low for the immunoprecipitation of the native AGO proteins. Thus, in order to examine AGO3–target RNA interactions by RNA-binding protein immunoprecipitation (RIP), we generated transgenic strains expressing FLAG-tagged AGO3 in the *vig1* and the Maa7-IR44 backgrounds. We selected transgenic strains expressing FLAG-AGO3 at similar levels and where the introduced tagged protein replaced a fraction of the endogenous AGO3, rather than overexpressing it to unphysiological levels [*SI Appendix*, Fig. S8*B*; Maa7-IR44(FLAG-AGO3)-56 and vig1(FLAG-AGO3)-31]. As in mammalian cells (33), AGO3/2 and (most) miRNA/siRNA levels are positively correlated in *C. reinhardtii* (19, 21), suggesting that AGO3/2 proteins are stabilized by association with sRNAs and vice versa. As a further indication that FLAG-AGO3 proteins were not exceedingly overexpressed, we also verified that the transgenic strains had similar levels of endogenous miRNAs and equivalent to those in the wild-type strain (*SI Appendix*, Fig. S8*C*). RIP from the selected strains and subsequent reverse-transcriptase (RT) PCR analysis revealed that FLAG-AGO3 binding to its target mRNAs was not appreciably defective in the *vig1* mutant (Fig. 5*C*). Hence, the association of AGO3-(mi)RISC with target RNAs is largely independent of VIG1.

Discussion

The biogenesis and function of sRNAs have been the subject of extensive research in diverse eukaryotes. There is now good evidence that, besides triggering mRNA degradation (in a slicer-dependent or -independent manner), the (mi)RISC can also cause translation repression of polyribosomal transcripts, in some cases without or with minimal mRNA destabilization, in animals, plants, and some protists like the alga *C. reinhardtii* (2, 4, 6, 11, 13). However, the actual mechanism(s) of this translation inhibition remains poorly characterized. As already mentioned, in metazoans, GW182/TNRC6 proteins are not required for this type of silencing and, in land plants, the factors implicated in translation repression do not provide clear insight into the molecular mechanism(s).

In mammalian cells, some CDS miRNA target sites comprise a new category of recognition elements, involving weak interactions with the miRNA seed (nucleotides 2 to 7) but extensive pairing with its 3′ half (11). The translationally repressed target transcripts containing these elements remain associated with translating ribosomes, without alteration in the overall ribosome occupancy (11). In *C. elegans*, *lin-41* mRNA also remains associated with ribosomes, without alterations in ribosome occupancy, despite strong translation repression by the let-7 miRNA in L4 larvae (13). Moreover, ribosomal profiles from repressed *lin-41* transcripts showed no evidence for either premature ribosomal dropoff or site-specific ribosome stalling as a possible mechanism of let-7–triggered silencing (13). In *D. melanogaster* S2 cells, an miRISC induced by serum starvation and causing enhanced translation repression associates with mRNAs assembled into polyribosomes (10). In *A. thaliana*, mRNAs targeted for miRNA-mediated translation inhibition are also associated with polyribosomes and the repression appears to occur in the ER (2, 4, 15). However, no ribosome pausing upstream of CDS miRNA-binding sites was observed in Ribo-seq or RNA degradome analyses (14, 18). In *Chlamydomonas*, we reported that transcripts translationally repressed by sRNAs also remain associated with polyribosomes without discernable changes in ribosome occupancy (6), and global ribosome profiling did not detect ribosome footprints piling up upstream of CDS miRNA binding sites (20). These observations suggest the existence of a similar mechanism of translation inhibition in widely divergent eukaryotes but how the (mi)RISC triggers repression in a polyribosomal context is not understood.

VIG/SERBP1 is an evolutionarily conserved eukaryotic protein (*SI Appendix*, Fig. S2). It was identified more than a decade ago as a component of the (mi)RISC in *D. melanogaster*, *C. elegans*, and human cells (24, 25) but its actual mechanistic role(s) has not been elucidated. In *C. elegans*, VIG1 is required for let-7–mediated repression of a lacZ-lin-41 reporter, but not for (cleavage-mediated) RNAi (24). Since the endogenous *lin-41* transcript is translationally repressed by let-7 while associated with polyribosomes (13), it seems plausible that VIG1 is involved in this process. However, *C. elegans vig1* mutants also show reduced levels of mature let-7 miRNAs, suggesting alternative (not mutually exclusive) VIG1 functions in miRISC loading and/or miRNA stability (25). Nonetheless, a growing body of evidence also supports the association of VIG/SERBP1 homologs with ribosomes. *S. cerevisiae* Stm1, *D. melanogaster* VIG2, and mammalian SERBP1 interact with inactive ribosomes as clamping factors that presumably prevent ribosome disassembly and decay when translation is inhibited by nutrient starvation/stress conditions (26–30). In addition, *S. cerevisiae* Stm1 and mammalian SERBP1 have been shown to associate with translating polyribosomes (30, 34, 35). Yeast Stm1 has been reported to perturb the association of elongation factor eEF3 with ribosomes and affect optimal translation elongation (34). Translation experiments using yeast extracts also suggested that Stm1 represses translation elongation, after formation of 80S ribosomes (30, 36). Additionally, yeast Stm1 has been genetically linked to mRNA decapping and degradation (30, 36). Mammalian SERBP1 has been implicated in multiple functions but recent findings indicate that most cytoplasmic SERBP1 is precipitated by ultracentrifugation and associates with translating ribosomes (as a substoichiometric component of the 40S subunit) (35). One of the *A. thaliana* VIG/SERBP1 homologs, *At*RGGA, localizes in the cytoplasm and the perinuclear region (consistent with an association with ribosomes, although this has not been examined) and is involved in plant responses to osmotic stress (37).

The association of VIG/SERBP1 homologs with translating ribosomes may be mediated, at least partly, by RACK1 (receptor of activated protein C kinase 1), which is a component of the 40S ribosomal subunit and also acts as a scaffold for many proteins involved in diverse signaling pathways (38, 39). In yeast 2-hybrid assays, mammalian SERBP1 interacts with RACK1 (40) and proximity-dependent biotin identification analyses suggest that *S. cerevisiae* Stm1 is deposited close to RACK1, within the 40S ribosomal head region, when mRNAs are actively translated (29). Interestingly, RACK1 has also been found to affect different aspects of the miRNA pathway, from biogenesis to effector functions, in plants and metazoans (38, 39, 41). In *C. elegans* and human cells, RACK1 copurifies with AGOs and has been proposed to facilitate the recruitment of the miRISC to the ribosome (41). RACK1 was also found in complexes with AGO1 in *A. thaliana*, although its potential role in an sRNA effector complex has not been examined (42).

Like some of its homologs, *Chlamydomonas* VIG1 localizes predominantly in the cytosol, with some preference for perinuclear regions (Fig. 4 and *SI Appendix*, Fig. S7), and comigrates with monoribosomes and polyribosomes by sucrose density gradient sedimentation (Fig. 5*A*). Affinity purification of FLAG-CBP-VIG1, from RNase A-treated cell lysates, indicated that the association of VIG1 with components of the translation machinery, including several translation initiation factors and ribosomal proteins, is RNA-independent (Fig. 3*A*). Moreover, the *vig1*-deleted mutant is hypersensitive to exposure to the translation elongation inhibitor cycloheximide (*SI Appendix*, Fig. S9*B*), suggesting that VIG1 may have some role(s) in ribosome function/structure. *Chlamydomonas* VIG1 also copurifies with AGO3 and DCL3 (Fig. 3*A*), consistent with it being a component of the (mi)RISC, and its depletion prevented the sRNA-mediated translation repression of polyribosomal transcripts (Figs. 1 and 2). However, this protein was dispensable for cleavage-mediated RNAi (*SI Appendix*, Fig. S4*A*) as well as for the association of the AGO3 effector with polyribosomes and with target transcripts (Fig. 5 *B* and *C*). Intriguingly, we have previously reported that ribosomes associated with sRNA-repressed transcripts showed reduced sensitivity to translation inhibition by cycloheximide and suggested that sRNA-mediated repression of protein synthesis in *C. reinhardtii* may involve alterations to the function/structural conformation of translating ribosomes (6). Together with current results, it is tempting to speculate that VIG1 is an ancillary ribosomal component and plays a direct role in the translation repression of siRNA/miRNA-targeted transcripts.

We hypothesize that the core (mi)RISC may interact (directly or indirectly) with *Chlamydomonas* VIG1 to trigger translation inhibition. Yet, VIG1 is predicted to be an intrinsically disordered protein (*SI Appendix*, Fig. S1*B*). This type of protein does not assume a single folded structure but instead rapidly interconverts between heterogeneous conformational states depending on environmental conditions and/or partner interactions (43, 44). Recent studies established that phase separation and protein–protein (and/or protein–RNA) interactions of a number of intrinsically disordered proteins are also regulated by posttranslational modifications, in particular arginine methylation and serine/threonine/tyrosine phosphorylation (43, 44). Indeed, the RG/RGG motifs (45) of VIG1, which are extensively methylated in arginine residues in mammalian SERBP1 (46), may conceivably be required for proper interaction with the core (mi)RISC and/or the actual translation repression. In *S. cerevisiae*, which has lost all core components of the RNAi machinery (47), the VIG1 homolog, Stm1, lacks RG/RGG repeats (*SI Appendix*, Fig. S1*A*), consistent with these motifs being related to an sRNA-associated function(s).

We propose a model of sRNA-mediated translation repression of polyribosomal transcripts whereby VIG1 is generally associated with ribosomes (*SI Appendix*, Fig. S11*A*) and may play a minor (nonessential) role(s) in modulating ribosome function/structure under normal growth conditions. In *S. cerevisiae*, Stm1 seems to influence the association of elongation factor eEF3 with ribosomes, a protein that both stimulates eEF1A-dependent binding of a cognate aminoacyl-tRNA to the ribosomal A site and facilitates the release of deacylated tRNA from the ribosomal E site (34, 48). Although eEF3 was initially thought to be a fungal-specific translation factor, eEF3-like (eEF3L) proteins have now been identified in a wider range of eukaryotes (49). *Chlamydomonas* encodes 2 eEF3L homologs, containing the conserved domains involved in the interactions of yeast eEF3 with eEF1A and with the ribosome near the E site (48, 49). Given the *vig1* mutant hypersensitivity to cycloheximide, VIG1 may possibly modulate translation elongation (e.g., by influencing the activity/interactions of eEF3L factors) and/or the accessibility of cycloheximide to its site of action at the ribosomal E site (32). Alternatively, VIG1 may associate with translating ribosomes mainly in "standby mode," until it is required for clamping ribosomal subunits under nutrient starvation (29). Upon core (mi) RISC binding to a target transcript in a polyribosomal context, we hypothesize that it interacts (directly or indirectly) with VIG1 and switches this protein into an alternative conformational state leading to translation repression at potentially multiple steps (*SI Appendix*, Fig. S11*B*). Since VIG1 copurifies with eIF3 subunits, which are known to associate with the 40S ribosomal subunit (29, 50), it could conceivably affect the recruitment/interaction of components of the translation initiation machinery. Additionally, VIG1 associated with translating 80S ribosomes could inhibit translation elongation, as reported for yeast Stm1 (30, 36). However, in an in vitro assay with rabbit reticulocyte lysates, mammalian SERBP1 was able to bind to multiple ribosomal complexes but did not interfere with translation initiation or elongation (51), possibly reflecting the proposed need of an interaction with the core (mi)RISC for (nonfungal) VIG1 homologs to trigger translation repression.

We favor the above model, characterized by an overall reduction (slowdown) of both translation initiation and elongation rates, because, in *Chlamydomonas*, ribosomes remain associated with sRNA-repressed transcripts, without noticeable changes in ribosome occupancy, and appear to be actively translating although with reduced sensitivity to inhibition by cycloheximide (6). Intriguingly, pretreatment of the mammalian ECV-304 cell line with cycloheximide also partly relieved the miRNA-mediated repression of a *Renilla* luciferase reporter (52). Yet, alternative models are also consistent with our observations. For instance, mRNA-bound ribosomes could be simultaneously frozen on the transcript, conceivably through liquid–liquid phase separation triggered by conformational changes in intrinsically disordered VIG1 interacting with the core (mi)RISC. Thus, the exact mechanism by which VIG1 may contribute to translation repression will require further investigation.

Materials and Methods

Culture Conditions, Transgenic Strains, and Mutants. Unless noted otherwise, *C. reinhardtii* cells were grown photoheterotrophically in Tris-acetate-phosphate medium or photoautotrophically in minimal high-salt (HS) medium (53, 54). For phenotypic analyses, cells grown to logarithmic phase in TAP or HS media were serially diluted, spotted on plates of the appropriate media (see figure legends), and incubated for 7 to 15 d under dim lights (6, 23, 54). Mutants and transgenic strains are described in *SI Appendix, Materials and Methods*.

RNA Analyses. Total cell RNA was purified with TRI Reagent (Molecular Research Center), following the manufacturer's instructions. For Northern blot analyses of mRNAs, the isolated RNA was separated by agarose/formaldehyde gel electrophoresis, blotted onto nylon membranes, and hybridized with ^{32}P-labeled probes (6, 21, 55). For small RNA analyses, total RNA samples were resolved on 15% polyacrylamide/7 M urea gels and electroblotted to Hybond-XL membranes (GE Healthcare) (6, 21, 55). Blots were hybridized with ^{32}P-labeled DNA probes at 40 °C for 48 h using the High Efficiency Hybridization System (Molecular Research Center). Specific miRNAs were detected by hybridization with complementary DNA oligonucleotides labeled at their 5′ termini with γ-[^{32}P]ATP and T4 polynucleotide kinase (6, 21). RNA-seq and Ribo-seq data for wild-type *C. reinhardtii* were reanalyzed from Chung et al. (56) (accession nos. ERX558436 and ERX558438).

Immunoblot Analyses. Approximately 5 × 10^6 cells, grown to logarithmic phase, were pelleted by centrifugation and resuspended in 50 μL of SDS gel-running buffer. Ten-microliter aliquots of boiled samples were separated by SDS/PAGE and electrophoretically transferred to nitrocellulose membranes (54, 55). Tryptophan synthase β-subunit was immunodetected by overnight incubation at 4 °C with a 1:5,000 dilution of a rabbit antibody raised against the *Camptotheca acuminata* enzyme (a generous gift from Thomas McKnight, Texas A&M University, College Station, Texas) (6, 21). AGO3 was detected by incubation with a 1:10,000 dilution of a rabbit antibody raised against a C-terminal peptide (ASRSGRGAGAAEGG) conjugated to keyhole limpet hemocyanin (KLH) (21). This antibody also cross-reacts with *Chlamydomonas* AGO2 (19), but the steady-state level of this protein is, at least,

1 order of magnitude lower than that of AGO3 [PaxDb (57)]. The Cre16.g683650 protein was immunodetected by overnight incubation at 4 °C with a 1:10,000 dilution of a rabbit antibody raised against a C-terminal peptide (GIKPSAHKRGGVRM) conjugated to KLH (22). Commercially available antibodies were used to detect histone H3 (Abcam; ab1791), RPL37 (Agrisera; AS12 2115), COX2B (Agrisera; AS06 151), RPS14 (Agrisera; AS12 2111), RBCS1/2 (Agrisera; AS07 259), and the AcV5 epitope tag (antibaculovirus envelope gp64 protein; eBioscience; 14-6995), which was engineered as part of the FLAG-CBP tag.

Affinity Purification of FLAG-CBP–Tagged VIG1 and Protein Identification by Mass Spectrometry. To purify VIG1-associated polypeptides, a complemented *vig1* transgenic strain [vig1(tagVIG1)-3] was grown to midlogarithmic phase in TAP medium (containing 7 μM 5-FI) and cells were collected by centrifugation. For each experiment, ~2×10^{10} cells were resuspended in lysis buffer (20 mM Tris·HCl, pH 7.5, 150 mM NaCl, 2 mM $Mg[CH_3COO]_2 \cdot 4H_2O$, 2.5 mM $CaCl_2$, 1 mM imidazole, 10 mM β-mercaptoethanol, and 10% glycerol) supplemented with 2.0 mM benzamidine, 0.2 mM phenylmethanesulfonyl fluoride (PMSF), 5 μL/mL plant protease inhibitor mixture (Sigma), and 30 μg/mL RNase A. Cells were broken by 2 passages through a French press at 5,000 psi and the lysate was clarified by centrifugation at 16,000 × *g* for 30 min at 4 °C. The extract was then incubated with buffer-equilibrated calmodulin-Sepharose beads (GE Healthcare) for 16 h at 4 °C. Subsequent purification steps were performed as previously described (58). FLAG-CBP-Ble purification, following the same protocol, was used as a negative control. Isolated proteins were fractionated by 10% SDS/PAGE, stained with Sypro Ruby (Bio-Rad), digested in-gel with trypsin, and identified by tandem mass spectrometry as described (58). We observed that VIG1 migrates anomalously on SDS/PAGE and appears larger than its predicted size, as previously reported for mammalian SERBP1 (35).

In Vitro RISC Activity. To test for sequence-specific cleavage activity, VIG1 and associated proteins were purified as described above. After the final regular wash, the beads were rewashed and resuspended with RISC activity buffer (30 mM Hepes, pH 7.5, 100 mM NaCl, 5 mM $Mg[CH_3COO]_2$, 2 mM $CaCl_2$, and 0.5 mM DTT). The in vitro reactions contained 17 μL resuspended beads in RISC activity buffer, 1 μL γ-^{32}P–labeled synthetic *MAA7* RNA (1 pmol/μL 5′-GACCAGCACUGUGCUUUGACAGACAAGCUCACGCG-3′; IDT), 1 μL 40 U/μL RNasin Plus (Promega), and 1 μL of a mixture of 0.2 mM GTP and 1 mM ATP (final volume 20 μL). For EDTA treatments, the reactions were supplemented with 8 mM EDTA. A nonhomologous, ^{32}P-labeled RNA (5′-GUGGAUUGAUCCCAGCCAGGCGAAA-3′; IDT) was also used as a negative-control substrate. All reactions were allowed to proceed at room temperature for 0, 20, or 40 min. At each time point, an aliquot was transferred to a new tube on ice and an equal volume of formamide loading buffer (55) was added. Stopped reactions were heated at 65 °C for 3 min, quickly cooled on ice, and 3 μL was then resolved on 15% denaturing polyacrylamide gels and detected by autoradiography.

Immunofluorescence Microscopy. Immunofluorescence microscopy of *Chlamydomonas* was performed with minor modifications to published protocols (59, 60). After allowing cells to adhere to polyethyleneimine-coated slides (Sigma), they were fixed using 4% paraformaldehyde in phosphate-buffered saline (PBS) for 30 min. Slides were then washed twice in −20 °C methanol for 10 min each. After rehydration in PBS, cells were further permeabilized with 0.5% Triton X-100 and rewashed in PBS. Fixed cells were then incubated in blocking buffer (10 mM K_2HPO_4/KH_2PO_4, pH 7.2, 5% glycerol, 1% BSA, 5% normal goat serum, 1% cold-water fish gelatin, and 0.04% sodium azide) for 2 h. After blocking, cells were incubated with 1:10,000 diluted primary anti-AcV5 antibody at 4 °C for 24 h. The secondary antibody, goat anti-mouse IgG conjugated to Alexa Fluor 488 (Invitrogen; A11001), was diluted 1:500 in blocking buffer and incubated with the cells for 2 h at room temperature. Following exposure to the secondary antibody, samples were stained with 5 μM DAPI, washed in PBS, and finally mounted with Gel Mount (Sigma). Cells were imaged using an Olympus FluoView 500 confocal laser-scanning microscope.

Polyribosome Profile Analyses. These experiments were carried out as previously described (6) and are briefly outlined in *SI Appendix, Materials and Methods*.

RNA-Binding Protein Immunoprecipitation. *C. reinhardtii* strains, expressing FLAG-AGO3 or FLAG-Ble, were grown to midlogarithmic phase in TAP medium, and ~4×10^9 cells were pelleted by centrifugation and resuspended in 10 mL of lysis buffer (50 mM Tris·HCl, pH 7.5, 120 mM NaCl, 2 mM benzamidine, 0.2 mM PMSF, and 10% glycerol) containing 5 μL/mL plant protease inhibitor mixture (Sigma). From this step on, cells and lysates were always kept on ice. Cells were broken by 2 passages through a French press at a pressure of ~2,000 psi. Cell lysates were then centrifuged at 16,000 × *g* for 30 min. CHAPS (0.1% final concentration) was added to the supernatant and an aliquot (~10%) was saved for input control analyses of proteins and RNAs. The remaining supernatant was incubated with buffer-equilibrated anti–FLAG-M2 agarose beads (Sigma) for 2 h, and then the beads were washed 5 times with lysis buffer containing 0.1% CHAPS and 5 μL/mL plant protease inhibitor mixture. Proteins/RNAs associated with the beads were eluted by incubation with lysis buffer (without glycerol) containing 150 μg/mL 3×FLAG peptide (Sigma). RNA was purified from the eluate, precipitated with glycogen as carrier, and used for RT-PCR analyses (55).

Reverse-Transcriptase PCR Analyses. First-strand cDNA synthesis and PCR reactions were performed as previously described (21, 54, 55). Specific details and primers are described in *SI Appendix, Materials and Methods*.

Data Availability. All data and protocols used to support the findings of this study have been included in the manuscript and *SI Appendix* or made available through the National Center for Biotechnology Information.

ACKNOWLEDGMENTS. This work was supported in part by a grant from the NSF (to H.C.). We thank Xiaoxue Wen for technical assistance with several immunoblotting experiments.

1. D. P. Bartel, Metazoan microRNAs. *Cell* **173**, 20–51 (2018).
2. Y. Yu, T. Jia, X. Chen, The 'how' and 'where' of plant microRNAs. *New Phytol.* **216**, 1002–1017 (2017).
3. L. F. R. Gebert, I. J. MacRae, Regulation of microRNA function in animals. *Nat. Rev. Mol. Cell Biol.* **20**, 21–37 (2019).
4. H. O. Iwakawa, Y. Tomari, The functions of microRNAs: mRNA decay and translational repression. *Trends Cell Biol.* **25**, 651–665 (2015).
5. T. F. Duchaine, M. R. Fabian, Mechanistic insights into microRNA-mediated gene silencing. *Cold Spring Harb. Perspect. Biol.* **11**, a032771 (2019).
6. X. Ma *et al.*, Small interfering RNA-mediated translation repression alters ribosome sensitivity to inhibition by cycloheximide in *Chlamydomonas reinhardtii*. *Plant Cell* **25**, 985–998 (2013).
7. A. Dallaire, P. M. Frédérick, M. J. Simard, Somatic and germline microRNAs form distinct silencing complexes to regulate their target mRNAs differently. *Dev. Cell* **47**, 239–247.e4 (2018).
8. J. W. Freimer, T. J. Hu, R. Blelloch, Decoupling the impact of microRNAs on translational repression versus RNA degradation in embryonic stem cells. *eLife* **7**, e38014 (2018).
9. R. S. Muddashetty *et al.*, Reversible inhibition of PSD-95 mRNA translation by miR-125a, FMRP phosphorylation, and mGluR signaling. *Mol. Cell* **42**, 673–688 (2011).
10. P. H. Wu, M. Isaji, R. W. Carthew, Functionally diverse microRNA effector complexes are regulated by extracellular signaling. *Mol. Cell* **52**, 113–123 (2013).
11. K. Zhang *et al.*, A novel class of microRNA-recognition elements that function only within open reading frames. *Nat. Struct. Mol. Biol.* **25**, 1019–1027 (2018).
12. H. Y. Jin, C. Xiao, MicroRNA mechanisms of action: What have we learned from mice? *Front. Genet.* **6**, 328 (2015).
13. M. Stadler, K. Artiles, J. Pak, A. Fire, Contributions of mRNA abundance, ribosome loading, and post- or peri-translational effects to temporal repression of *C. elegans* heterochronic miRNA targets. *Genome Res.* **22**, 2418–2426 (2012).
14. C. Y. Hou *et al.*, Global analysis of truncated RNA ends reveals new insights into ribosome stalling in plants. *Plant Cell* **28**, 2398–2416 (2016).
15. S. Li *et al.*, MicroRNAs inhibit the translation of target mRNAs on the endoplasmic reticulum in *Arabidopsis*. *Cell* **153**, 562–574 (2013).
16. R. S. Reis, G. Hart-Smith, A. L. Eamens, M. R. Wilkins, P. M. Waterhouse, Gene regulation by translational inhibition is determined by Dicer partnering proteins. *Nat. Plants* **1**, 14027 (2015).
17. H. O. Iwakawa, Y. Tomari, Molecular insights into microRNA-mediated translational repression in plants. *Mol. Cell* **52**, 591–601 (2013).
18. M. J. Liu *et al.*, Translational landscape of photomorphogenic *Arabidopsis*. *Plant Cell* **25**, 3699–3710 (2013).
19. T. Yamasaki, E. J. Kim, H. Cerutti, T. Ohama, Argonaute3 is a key player in miRNA-mediated target cleavage and translational repression in *Chlamydomonas*. *Plant J.* **85**, 258–268 (2016).
20. B. Y. Chung, M. J. Deery, A. J. Groen, J. Howard, D. C. Baulcombe, Endogenous miRNA in the green alga *Chlamydomonas* regulates gene expression through CDS-targeting. *Nat. Plants* **3**, 787–794 (2017).
21. F. Ibrahim *et al.*, Uridylation of mature miRNAs and siRNAs by the MUT68 nucleotidyltransferase promotes their degradation in *Chlamydomonas*. *Proc. Natl. Acad. Sci. U.S.A.* **107**, 3906–3911 (2010).

PLANT BIOLOGY

22. A. Voshall, E. J. Kim, X. Ma, E. N. Moriyama, H. Cerutti, Identification of AGO3-associated miRNAs and computational prediction of their targets in the green alga *Chlamydomonas reinhardtii*. *Genetics* **200**, 105–121 (2015).
23. A. Voshall *et al*., miRNAs in the alga *Chlamydomonas reinhardtii* are not phylogenetically conserved and play a limited role in responses to nutrient deprivation. *Sci. Rep.* **7**, 5462 (2017).
24. A. A. Caudy *et al*., A micrococcal nuclease homologue in RNAi effector complexes. *Nature* **425**, 411–414 (2003).
25. C. Wang *et al*., TEG-1 CD2BP2 controls miRNA levels by regulating miRISC stability in *C. elegans* and human cells. *Nucleic Acids Res.* **45**, 1488–1500 (2017).
26. A. M. Anger *et al*., Structures of the human and *Drosophila* 80S ribosome. *Nature* **497**, 80–85 (2013).
27. A. Brown, M. R. Baird, M. C. Yip, J. Murray, S. Shao, Structures of translationally inactive mammalian ribosomes. *eLife* **7**, e40486 (2018).
28. N. Van Dyke, E. Chanchorn, M. W. Van Dyke, The *Saccharomyces cerevisiae* protein Stm1p facilitates ribosome preservation during quiescence. *Biochem. Biophys. Res. Commun.* **430**, 745–750 (2013).
29. N. Opitz *et al*., Capturing the Asc1p/receptor for activated C kinase 1 (RACK1) microenvironment at the head region of the 40S ribosome with quantitative BioID in yeast. *Mol. Cell. Proteomics* **16**, 2199–2218 (2017).
30. H. Hayashi *et al*., Tight interaction of eEF2 in the presence of Stm1 on ribosome. *J. Biochem.* **163**, 177–185 (2018).
31. M. M. Kucherenko, H. R. Shcherbata, miRNA targeting and alternative splicing in the stress response—Events hosted by membrane-less compartments. *J. Cell Sci.* **131**, jcs202002 (2018).
32. S. Klinge, F. Voigts-Hoffmann, M. Leibundgut, S. Arpagaus, N. Ban, Crystal structure of the eukaryotic 60S ribosomal subunit in complex with initiation factor 6. *Science* **334**, 941–948 (2011).
33. P. Smibert, J. S. Yang, G. Azzam, J. L. Liu, E. C. Lai, Homeostatic control of Argonaute stability by microRNA availability. *Nat. Struct. Mol. Biol.* **20**, 789–795 (2013).
34. N. Van Dyke, B. F. Pickering, M. W. Van Dyke, Stm1p alters the ribosome association of eukaryotic elongation factor 3 and affects translation elongation. *Nucleic Acids Res.* **37**, 6116–6125 (2009).
35. A. Muto *et al*., The mRNA-binding protein Serbp1 as an auxiliary protein associated with mammalian cytoplasmic ribosomes. *Cell Biochem. Funct.* **36**, 312–322 (2018).
36. V. Balagopal, R. Parker, Stm1 modulates translation after 80S formation in *Saccharomyces cerevisiae*. *RNA* **17**, 835–842 (2011).
37. A. Ambrosone *et al*., The *Arabidopsis* RNA-binding protein AtRGGA regulates tolerance to salt and drought stress. *Plant Physiol.* **168**, 292–306 (2015).
38. T. Islas-Flores, A. Rahman, H. Ullah, M. A. Villanueva, The receptor for activated C kinase in plant signaling: Tale of a promiscuous little molecule. *Front. Plant Sci.* **6**, 1090 (2015).
39. C. Speth, S. Laubinger, RACK1 and the microRNA pathway: Is it déjà-vu all over again? *Plant Signal. Behav.* **9**, e27909 (2014).
40. G. B. Bolger, The RNA-binding protein SERBP1 interacts selectively with the signaling protein RACK1. *Cell. Signal.* **35**, 256–263 (2017).
41. G. Jannot *et al*., The ribosomal protein RACK1 is required for microRNA function in both *C. elegans* and humans. *EMBO Rep.* **12**, 581–586 (2011).
42. C. Speth, E. M. Willing, S. Rausch, K. Schneeberger, S. Laubinger, RACK1 scaffold proteins influence miRNA abundance in *Arabidopsis*. *Plant J.* **76**, 433–445 (2013).
43. P. A. Chong, R. M. Vernon, J. D. Forman-Kay, RGG/RG motif regions in RNA binding and phase separation. *J. Mol. Biol.* **430**, 4650–4665 (2018).
44. M. Hofweber, D. Dormann, Friend or foe—Post-translational modifications as regulators of phase separation and RNP granule dynamics. *J. Biol. Chem.* **294**, 7137–7150 (2019).
45. P. Thandapani, T. R. O'Connor, T. L. Bailey, S. Richard, Defining the RGG/RG motif. *Mol. Cell* **50**, 613–623 (2013).
46. Y. J. Lee, W. Y. Hsieh, L. Y. Chen, C. Li, Protein arginine methylation of SERBP1 by protein arginine methyltransferase 1 affects cytoplasmic/nuclear distribution. *J. Cell. Biochem.* **113**, 2721–2728 (2012).
47. H. Cerutti, J. A. Casas-Mollano, On the origin and functions of RNA-mediated silencing: From protists to man. *Curr. Genet.* **50**, 81–99 (2006).
48. C. B. Andersen *et al*., Structure of eEF3 and the mechanism of transfer RNA release from the E-site. *Nature* **443**, 663–668 (2006).
49. V. Murina *et al*., ABCF ATPases involved in protein synthesis, ribosome assembly and antibiotic resistance: Structural and functional diversification across the tree of life. *J. Mol. Biol.* **431**, 3568–3590 (2019).
50. L. S. Valášek *et al*., Embraced by eIF3: Structural and functional insights into the roles of eIF3 across the translation cycle. *Nucleic Acids Res.* **45**, 10948–10968 (2017).
51. A. Zinoviev, C. U. T. Hellen, T. V. Pestova, Multiple mechanisms of reinitiation on bicistronic calicivirus mRNAs. *Mol. Cell* **57**, 1059–1073 (2015).
52. A. Detzer, C. Engel, W. Wünsche, G. Sczakiel, Cell stress is related to re-localization of Argonaute 2 and to decreased RNA interference in human cells. *Nucleic Acids Res.* **39**, 2727–2741 (2011).
53. E. H. Harris, *The Chlamydomonas Sourcebook: Introduction to Chlamydomonas and Its Laboratory Use* (Academic Press, San Diego, 2009).
54. J. Rohr, N. Sarkar, S. Balenger, B. R. Jeong, H. Cerutti, Tandem inverted repeat system for selection of effective transgenic RNAi strains in *Chlamydomonas*. *Plant J.* **40**, 611–621 (2004).
55. J. Sambrook, D. W. Russell, *Molecular Cloning: A Laboratory Manual* (Cold Spring Harbor Laboratory Press, Cold Spring Harbor, NY, 2001).
56. B. Y. Chung *et al*., The use of duplex-specific nuclease in ribosome profiling and a user-friendly software package for Ribo-seq data analysis. *RNA* **21**, 1731–1745 (2015).
57. M. Wang, C. J. Herrmann, M. Simonovic, D. Szklarczyk, C. von Mering, Version 4.0 of PaxDb: Protein abundance data, integrated across model organisms, tissues, and cell-lines. *Proteomics* **15**, 3163–3168 (2015).
58. J. S. Rohila, M. Chen, R. Cerny, M. E. Fromm, Improved tandem affinity purification tag and methods for isolation of protein heterocomplexes from plants. *Plant J.* **38**, 172–181 (2004).
59. M. A. Sanders, J. L. Salisbury, Immunofluorescence microscopy of cilia and flagella. *Methods Cell Biol.* **47**, 163–169 (1995).
60. J. Uniacke, D. Colón-Ramos, W. Zerges, FISH and immunofluorescence staining in *Chlamydomonas*. *Methods Mol. Biol.* **714**, 15–29 (2011).